Experimental Neurology 362 (2023) 114319

Contents lists available at ScienceDirect

Experimental Neurology

journal homepage: www.elsevier.com/locate/yexnr

Research paper

The cannabinoid CB_1 receptor interacts with the angiotensin AT_2 receptor. Overexpression of AT_2-CB_1 receptor heteromers in the striatum of 6-hydroxydopamine hemilesioned rats

Rafael Rivas-Santisteban[a,b], Jaume Lillo[a,b], Iu Raïch[a,b], Ana Muñoz[b,c], Alejandro Lillo[a,b], Ana I. Rodríguez-Pérez[b,c], José L. Labandeira-García[b,c], Gemma Navarro[a,b,e,**], Rafael Franco[b,d,f,*]

[a] Department of Biochemistry and Physiology, School of Pharmacy and Food Science, Universitat de Barcelona, Barcelona, Spain
[b] CiberNed. Network Center for Neurodegenerative diseases, National Spanish Health Institute Carlos III, Madrid, Spain
[c] Laboratory of Cellular and Molecular Neurobiology of Parkinson's Disease, Research Center for Molecular Medicine and Chronic Diseases (CIMUS), Department of Morphological Sciences, Health Research Institute of Santiago de Compostela (IDIS), University of Santiago de Compostela, Santiago de Compostela, Spain
[d] Molecular Neurobiology laboratory, Department of Biochemistry and Molecular Biomedicine, Faculty of Biology, Universitat de Barcelona, Barcelona, Spain
[e] Neurosciences Institute, University of Barcelona (NeuroUB), Facultad de Psicología Campus de Mundet Paseo de la Vall d'Hebron, 171 08035 Barcelona, Spain
[f] School of Chemistry, Universitat de Barcelona, Barcelona, Spain

ARTICLE INFO

Keywords:
Cannabinoids
Parkinson's disease
G protein-coupled receptors
Pharmacology
Receptor heteromer

ABSTRACT

It is of particular interest the potential of cannabinoid and angiotensin receptors as targets in the therapy of Parkinson's disease (PD). While endocannabinoids are neuromodulators that act through the CB_1 and CB_2 cannabinoid receptors, the renin angiotensin-system is relevant for regulation of the correct functioning of several brain circuits. Resonance energy transfer assays in a heterologous system showed that the CB_1 receptor (CB_1R) can directly interact with the angiotensin AT_2 receptor (AT_2R). Coactivation of the two receptors results in increased G_i-signaling. The AT_2-CB_1 receptor heteromer imprint consists of a blockade of AT_2R-mediated signaling by rimonabant, a CB_1R antagonist. Interestingly, the heteromer imprint, discovered in the heterologous system, was also found in primary striatal neurons thus demonstrating the expression of the heteromer in these cells. In situ proximity ligation assays confirmed the occurrence of AT_2-CB_1 receptor heteromers in striatal neurons. In addition, increased expression of the AT_2-CB_1 receptor heteromeric complexes was detected in the striatum of a rodent PD model consisting of rats hemilesioned using 6-hydroxydopamine. Expression of the heteromer was upregulated in the striatum of lesioned animals and, also, of lesioned animals that upon levodopa treatment became dyskinetic. In contrast, there was no upregulation in the striatum of lesioned rats that did not become dyskinetic upon chronic levodopa treatment. The results suggest that therapeutic developments focused on the CB_1R should consider that this receptor can interact with the AT_2R, which in the CNS is involved in mechanisms related to addictive behaviors and to neurodegenerative and neuroinflammatory diseases.

Abbreviation: 6-OHDA, 6-hydroxydopamine; ACEA, arachidonyl-2′-chloroethylamide; AT_2R, Angiotensin AT_2 receptor; BRET, Bioluminescence Resonance Energy Transfer; CNS, Central Nervous System; CB_1R, Cannabinoid CB_1 receptor; ECB, Endocannabinoid; FBS, Fetal bovine serum; HEK, Human Embryonic Kidney; L-DOPA, levodopa; PD, Parkinson's disease; PEI, PolyEthylenImine; PLA, Proximity Ligation Assay; RLUC, Renilla luciferase; σ_1R, sigma$_1$ receptor; YFP, Yellow fluorescent protein.

* Correspondence to: R. Franco, Molecular Neurobiology laboratory, Department of Biochemistry and Molecular Biomedicine, Faculty of Biology, Universitat de Barcelona, Avinguda Diagonal 643, 08028 Barcelona, Spain.
** Correspondence to: G. Navarro, Department of Biochemistry and Physiology, School of Pharmacy and Food Science, Universitat de Barcelona, Av. de Joan XXIII, 27-31, 08028 Barcelona, Spain.
E-mail addresses: g.navarro@ub.edu (G. Navarro), rfranco@ub.edu (R. Franco).

https://doi.org/10.1016/j.expneurol.2023.114319
Received 2 October 2022; Received in revised form 14 December 2022; Accepted 6 January 2023
Available online 9 January 2023

1. Introduction

Endocannabinoids (ECBs) are important regulators of neurotransmission and other events that take place in the CNS in both health and disease. The action of ECBs is mediated by two receptors, CB_1 and CB_2, which belong to class A or rhodopsin-like G protein-coupled receptors (GPCR). Both are coupled to heterotrimeric G_i proteins and, consequently, their activation by ECBs, by phytocannabinoids or by synthetic cannabinoids causes the inhibition of adenylate cyclase and the decrease in cAMP levels (Alexander et al., 2021; Pertwee et al., 2010). The CB_1 receptor (CB_1R) is among the more abundant GPCRs on CNS neurons and has been considered a target for a variety of neurological diseases (Basavarajappa et al., 2017; de Lago and Fernández-Ruiz, 2007; Fernández-Ruiz et al., 2015b). The CB_2 receptor (CB_2R), less abundant in neurons, is expressed in glia and is also considered a target of diseases such as the hypoxia of the neonate (Castillo et al., 2010; Fernández-López et al., 2007; Franco et al., 2019; Pazos et al., 2013).

Interestingly, cannabinoids interact and regulate the functionality of non-cannabinoid receptors such as GPR55 and GPR18. It is intriguing why those receptors, which also belong to the GPCR family, are able to interact with cannabinoid CB_1 and/or CB_2 receptors (Martínez-Pinilla et al., 2020; Martínez-Pinilla et al., 2019; Martínez-Pinilla et al., 2014; Reyes-Resina et al., 2018). The heteromers resulting from the interaction of two different GPCRs endow each of the receptors that participate in the interaction with greater versatility and functionality. Indeed, GCPR heteromers display properties that are different from those displayed by individually expressed receptors (Franco et al., 2016). In addition, the real targets of certain therapeutic drugs are GPCR heteromers. In this context, we have been interested in knowing if the components of the cannabinoid system interact physically and/or functionally with the components of the renin-angiotensin system (RAS).

The RAS has been extensively studied in the periphery, and basic research went translational with the approval of antihypertensive drugs that target angiotensin II receptors (Conlin, 2000). More recently, the relevant role of RAS for higher functions has been revealed (see (Jackson et al., 2018; Urmila et al., 2021; Halbach O. and Albrecht, 2006; Wright and Harding, 2013) for review). Several years ago, angiotensin II receptors were identified in different regions of the human brain using a radioligand binding approach (Barnes et al., 1993). By imaging techniques in samples from human and non-human primates, angiotensin II receptors, type 1 and 2, have been identified in neurons of the substantia nigra, (Garrido-Gil et al., 2013) and striatum (Garrido-Gil et al., 2017), where they significantly contribute to motor control. In humans, a recent report demonstrates that high expression of the AT1 gene (AGTR1) characterizes the most vulnerable dopaminergic neurons in Parkinson's disease (PD) (Kamath et al., 2022; Labandeira-Garcia and Parga, 2022). Furthermore, GABAergic neurotransmission is modulated by angiotensin-II in the mouse substantia nigra (Singh et al., 2021).

The angiotensin II type 2 receptor (AT_2R) expressed in cells of the substantia nigra is attracting interest due to its involvement in neuroinflammation and neurodegeneration, and in neuropathological events related to aging (Rodriguez-Perez et al., 2020). A recent report highlights the participation of these receptors in the production of inflammatory cytokines by microglia (Garrido-Gil et al., 2022). The receptor is also in the focus of investigations related to neurodegenerative diseases and, in particular, PD, which results from the death of nigral dopaminergic neurons and is accompanied by neuroinflammation. Angiotensin receptor antagonists have been proposed in the therapy of PD (Jo et al., 2022; Lin et al., 2022), those drugs would act through a molecular mechanism that involves angiotensin II receptors expressed in neurons and glial cells (Labandeira-Garcia et al., 2021; Labandeira-Garcia et al., 2013; Perez-Lloret et al., 2017; Quijano et al., 2022; Rodriguez-Perez et al., 2018).

The aim of this paper was to address whether the CB_1R may interact with the AT_2R and the functional consequences of the interaction. The functionality of the receptors in the heteromeric environment was evaluated in a heterologous system where a heteromeric imprint was found for the AT_2-CB_1 receptor complexes. Heteromer imprint was also found in primary striatal neurons. Once demonstrated the expression of the CB_1R-AT_2R heteromer in striatal neurons we also addressed its upregulation/downregulation in striatal sections from the brain of i) a rat model of PD treated with vehicle, ii) a rat model of PD treated with levodopa (L-DOPA) without displaying dyskinesia and iii) a rat model of PD treated with L-DOPA and displaying dyskinesia. Dyskinesia being a common side effect of the treatment of PD patients with L-DOPA unbalances the motor control circuits by mechanisms that are not fully elucidated but that involve both renin-angiotensin and cannabinoid systems (Junior et al., 2020; Rivas-Santisteban et al., 2021).

2. Results

2.1. Direct interaction of the cannabinoid CB_1 receptor and the angiotensin AT_2 receptor

Due to the fact that it has been reported an interaction between the CB_2R and the angiotensin II type-1 receptor (AT_1R) (Rozenfeld et al., 2011), we aimed at assessing whether the cannabinoid receptor may also interact with the angiotensin II type-2 receptor (AT_2R). Immunocytochemistry assays were performed in HEK-293 T cells coexpressing the CB_1R fused to YFP and the AT_2R fused to Rluc (Fig. 1A-D). CB_1-YFP was detected by the YFP green fluorescence (green, A) and AT_1R-Rluc was detected by a mouse monoclonal anti-Rluc antibody and a secondary sulfo-cyanine3 (Cy3)-conjugated anti-mouse IgG antibody (red, B). Nuclei were blue-stained with Hoechst (Fig. 1C). Images in Fig. 1 were obtained at the lower planes, where cell plasma membrane extends on the glass of the slide; results in Fig. 1D indicate that receptors colocalize at the plasma membrane in contact with the slide and intracellularly. Colocalization at the plasma membrane was significant, as observed in yellow.

As colocalization does not demonstrate direct interaction, bioluminescence resonance energy transfer (BRET) assays were carried out in HEK-293 T cells expressing a constant amount of AT_2R-Rluc and increasing amounts of either CB_1R-YFP or σ_1R-YFP, a fusion protein consisting of sigma1 receptor (σ_1R) and YFP. For AT_2R-Rluc and CB_1R-YFP a BRET saturation curve was found; the parameters were $BRET_{max} = 35 \pm 3$ mBU and $BRET_{50} = 5 \pm 1$ (Fig. 2A). A linear relationship was obtained indicating a lack of interaction when using AT_2-Rluc and σ_1R-YFP (Fig. 2B). These results show that in a heterologous system the CB_1R interacts with the AT_2R but not with the σ_1R.

2.2. Functionality of CB_1 and AT_2 receptors in single transfected and cotransfected cells

To assess whether heteromerization confers any differential functional property comparing with that of receptors that are not forming heteromers, signaling assays were performed in cells expressing one receptor and in cells coexpressing the two receptors. As the AT_2R couples to G_i protein, thus leading to inhibition of adenylate cyclase and decreased intracellular cAMP levels, the concentration of this second messenger was measured in cells expressing AT_2Rs treated with forskolin (FK) and a selective AT_2R agonist, CGP-42112A. The agonist treatment reduced the cAMP levels that were previously raised by FK (Fig. 3A) and the effect was specific because it was completely blocked by pretreatment with the selective AT_2R antagonist, PD123319. Similar experiments were performed in cells expressing the CB_1R, which also couples to G_i. The reduction of forskolin-induced cAMP levels by arachidonyl-2′-chloroethylamide (ACEA), a selective agonist, was blocked by rimonabant, a selective CB_1R antagonist (Fig. 3B). When similar assays were performed in cells coexpressing both, the AT_2R and the CB_1R, the agonists of the two receptors exerted a significant effect that was reverted by the corresponding antagonists (Fig. 3C). In

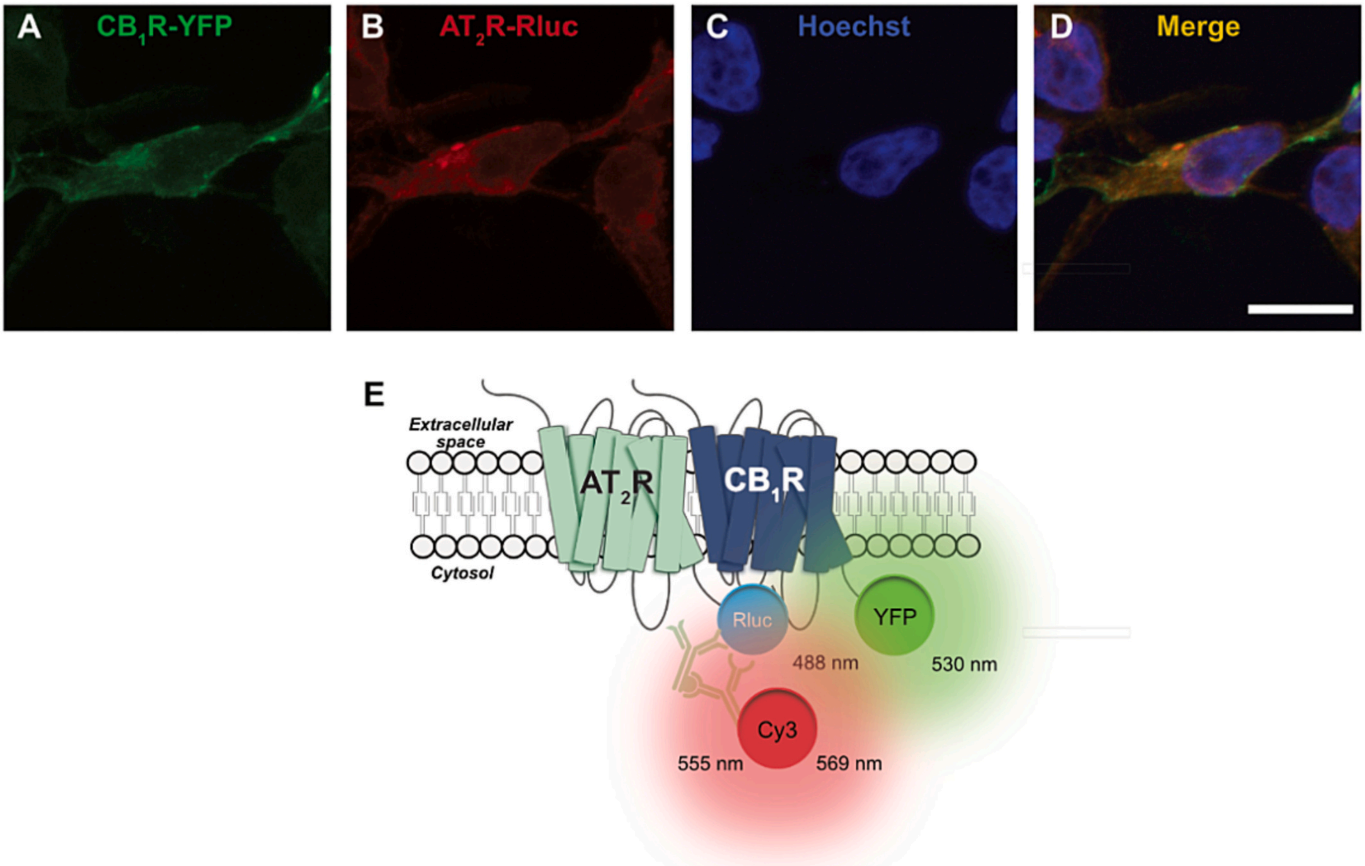

Fig. 1. Colocalization assays in a heterologous expression system. Immunocytochemistry assays were performed in HEK-293 T cells expressing AT_2R-Rluc (B, 1 μg cDNA) and CB_1R-YFP (A, 1 μg cDNA). CB_1R-YFP was detected by the YFP fluorescence (green). The Rluc-containing fusion protein was detected using a mouse monoclonal anti-Rluc antibody and a secondary Cy3-conjugated anti-mouse IgG antibody (red). Cell nuclei were stained with Hoechst (C, blue). Colocalization is shown in yellow (D). Confocal images were obtained at lower planes, where plasma membrane extends on the glass of the slide. Scheme of the design of immunocytochemistry assay is shown in E. Scale bar: 15 μm. (For interpretation of the references to colour in this figure legend, the reader is referred to the web version of this article.)

cotransfected cells, simultaneous activation of the two receptors led to a robust signal, which was higher than the response obtained by individual agonist treatment (Fig. 3C). In addition, the CB_1R antagonist rimonabant not only blocked the CB_1R-mediated effect but also that exerted by the AT_2R agonist. This is a phenomenon known as cross-antagonism and it was unidirectional as the AT_2R antagonist did not block the effect of the CB_1R agonist (Fig. 3C).

Using the imaging technique described in Methods, β-arrestin II recruitment was analyzed. For basal β-arrestin II recruitment detection, HEK-293 T cells expressing CB_1R were treated with vehicle before fixation and imaging; subsequent analysis of the images led to a Pearson's coefficient of approximately 0.2 (Fig. 4A). In single transfected cells each receptor agonist was able to recruit β-arrestin II to the plasma membrane (Fig. 4). Recruitment in cotransfected cells simultaneously treated with the two agonists (Fig. 4D) led to a significantly higher recruitment as indicated by the higher Pearson's coefficient: >0.6 versus <0.4 in single transfected cells (Fig. 4B, C).

2.3. Expression of AT_2-CB_1 receptor heteromers in mouse primary striatal neurons

The in situ proximity ligation assay (PLA) is instrumental to detect protein-protein interactions in cells and tissues. We took advantage of the technique to assess the expression of AT_2-CB_1 receptor heteromers in striatal neurons. Primary cultures were isolated from the striatum of fetuses as described in Methods. Experiments were performed using two specific antibodies, one against the CB_1R and another against the AT_2R. When one of the primary antibodies was omitted (negative control) a negligible signal was obtained (≈0.5 red dots/ cell). The presence of red fluorescent dots in the images obtained using antibodies against CB_1R and against AT_2R (Fig. 5) proves the occurrence of heteromers in primary neurons (≈9 red dots by cell). Labeling with Alexa Fluor®488 conjugated anti-NeuN antibody confirmed that heteromers were expressed in neurons (Fig. 5C).

2.4. Functionality of CB_1 and AT_2 receptors in mouse primary striatal neurons

cAMP determination assays were performed in primary striatal neurons treated with ACEA, CGP-42112A or both agonists. The results were similar to those found in HEK-293 T cells coexpressing AT_2 and CB_1 receptors. The reduction in FK-induced cAMP levels exerted by each agonist was additive/synergistic in the combined treatment (Fig. 6). Also, the cross-antagonism, i.e. rimonabant being able to block the effect of both ACEA and the AT_2R agonist, was detected as in the heterologous system (Fig. 6). Such cross-antagonism is an imprint that shows that AT_2-CB_1 receptor complexes occur in primary striatal neurons, confirming the PLA results shown in Fig. 5.

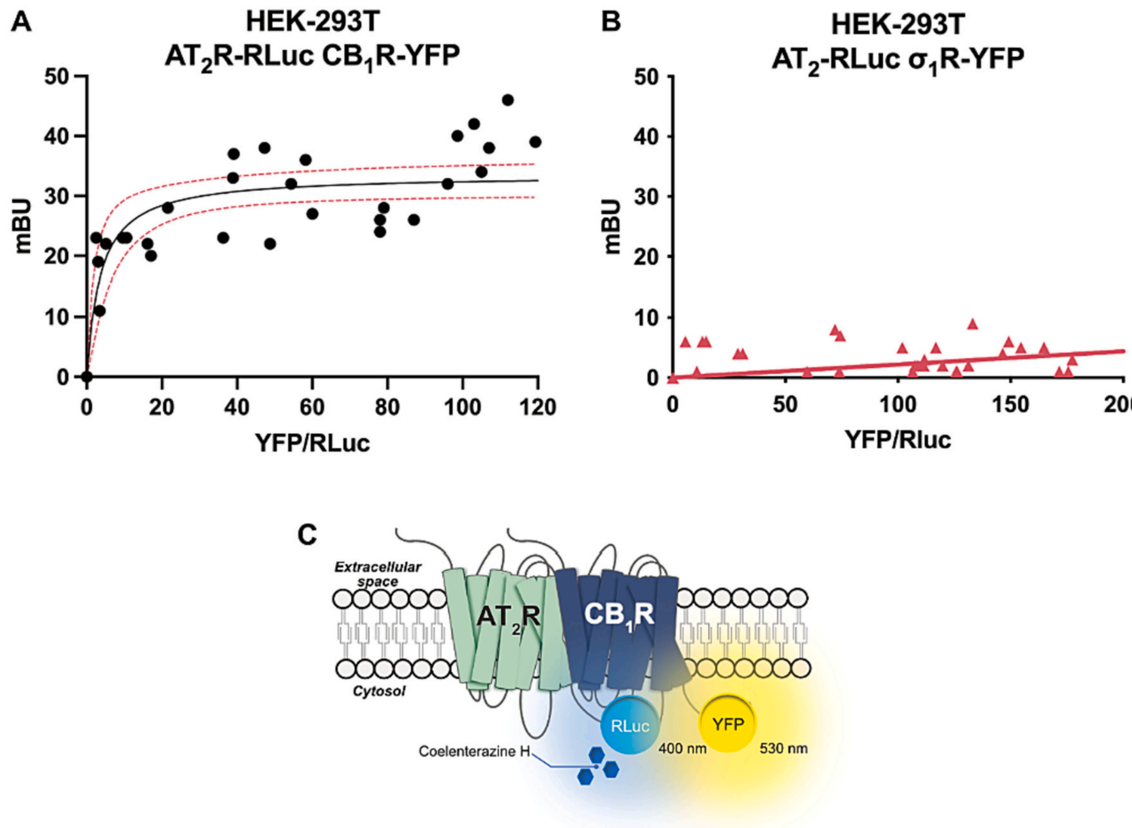

Fig. 2. AT_2R-CB_1R interaction detected by Bioluminescence Resonance Energy Transfer (BRET) in transfected HEK-293 T cells. Assays were performed in HEK-293 T cells transfected with a constant amount of cDNA for AT_2R-Rluc (1.2 μg) and increasing amounts of cDNA for CB_1R-YFP (0.33 to 1.5 μg) (panel A) or increasing amounts of cDNA for σ_1R-YFP (0.25 to 2.5 μg) (Panel B). The values shown in each graph were obtained in 6 independent experiments. Scheme of AT_2R-Rluc / CB_1R-YFP BRET assay is shown in C.

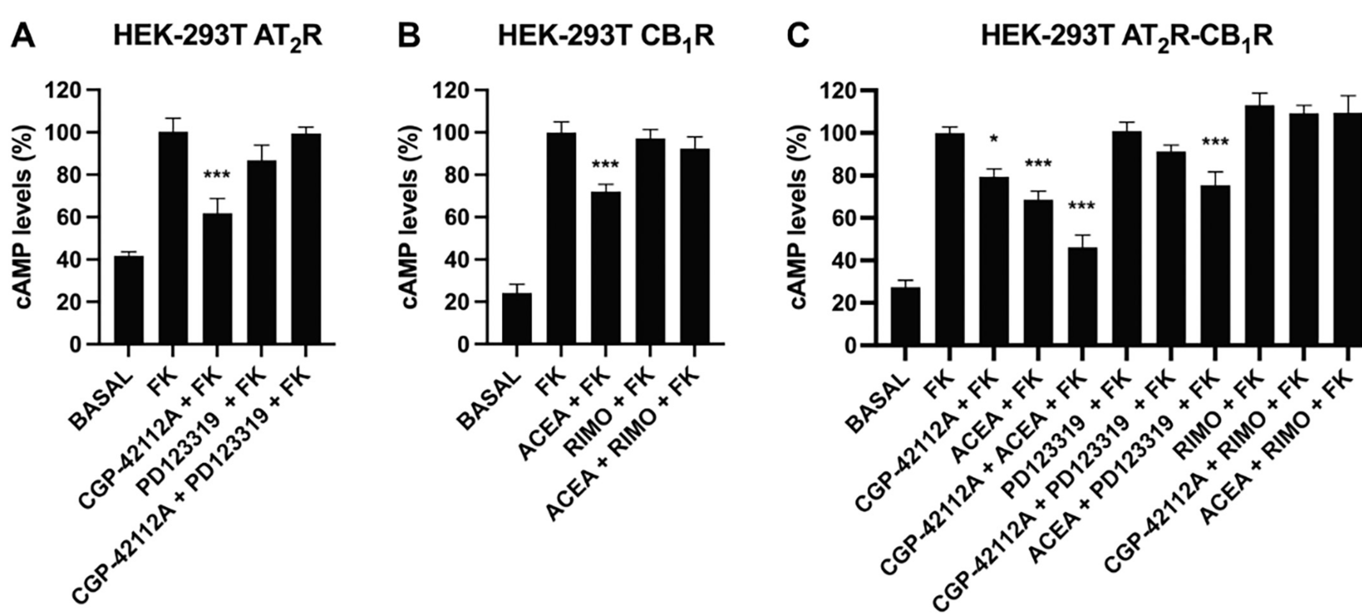

Fig. 3. Receptor functionality in single transfected and in cotransfected HEK-293 T cells. Cells expressing one (panels A, B) or the two (panel C) receptors were pretreated for 15 min with vehicle or selective antagonists: PD123319 for the AT_2R or rimonabant (RIMO) for the CB_1R. Activation of receptors (15 min) was performed with agonists: CGP-42112A for the AT_2R or ACEA for the CB_1R. Finally, cells were treated for an additional 15 min with 0.5 μM forskolin (FK). cAMP levels were determined as described in methods. Values are the mean ± S.E.M. of 5 different experiments performed in triplicates. Values are expressed as percentage of cAMP accumulation provoked by FK ($n = 5$, in triplicates). One-way ANOVA followed by Bonferroni's multiple comparison tests were used for statistical analysis. $^{*}p < 0.05$; $^{***}p < 0.001$ versus FK treatment.

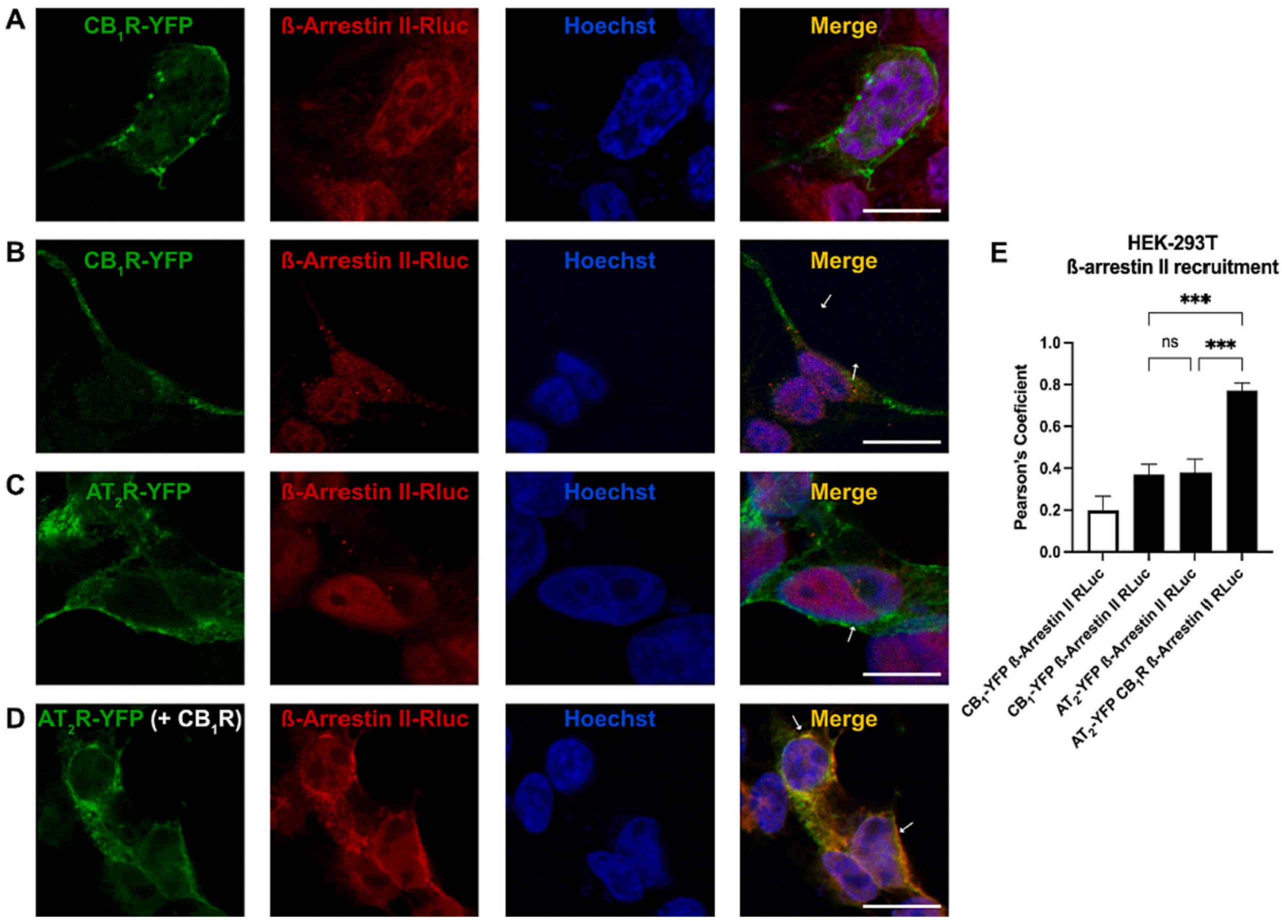

Fig. 4. β-arrestin II recruitment in HEK-293 T cells expressing AT_2R-YFP, CB_1R-YFP or both receptors. Panels A to D, confocal images were obtained in HEK-293 T cells expressing ß-arrestin II-Rluc and AT_2R-YFP and/or CB_1R-YFP. Cells were fixed with paraformaldehyde (4%) after adding receptor agonists for 5 min of adding: vehicle in CB_1R-YFP-expressing cells (panel A), ACEA in CB_1R-YFP-expressing cells (Panel B), CGP-42112A in AT_2R-YFP-expressing cells (Panel C) or CGP-42112A and ACEA in cells coexpressing AT_2R-YFP and CB_1R-YFP (Panel D). ß-arrestin II recruitment was analyzed by determining the colocalization of the fluorescence signal between the YFP-labeled receptor and ß-arrestin II-Rluc labeled with a sulfo-cyanine3 (Cy3)-conjugated antibody. For this purpose, the Pearson's correlation coefficient was calculated with Fiji software by processing the images obtained in the confocal as described in methods. Values in the bars graph are the mean ± S.E.M. of 5 different experiments. One-way ANOVA and Bonferroni's multiple comparison *post-hoc* tests were used for statistical analysis $***p < 0.001$. Scale bar: 15 μm.

2.5. Expression of AT_2 and CB_1 receptor heteromers in brain striatal sections of the PD rat model

Due to the relevance of alterations of the renin-angiotensin system in PD, a final aim was to determine the expression of the AT_2R-CB_1R heteromer in the striatum of healthy animals and of three groups of lesioned animals: 6-hydroxydopamine (6-OHDA)-lesioned animals receiving vehicle, 6-OHDA-lesioned animals receiving a chronic treatment with L-DOPA and divided into those that were not dyskinetic and those that were rendered dyskinetic upon chronic L-DOPA treatment. PLA assays in brain sections containing the striatum were performed simultaneously and in identical conditions to detect the occurrence of AT_2R-CB_1R heteromers and for level quantitation. A representative image obtained using brains of each of the animal groups is shown in Fig. 7A-D; quantitation, expressed as a ratio of red dots in cells having dots, is shown in the form of bar graph in Fig. 7E. While the number of detected AT_2R-CB_1R complexes was already remarkably high in the striatum of non-lesioned rats (circa 7 red dots/cell), the striatum of lesioned animals showed significantly more heteromers (circa 9 red dots/cell). The levels returned to normal, i.e. to the levels found in non-lesioned animals, upon L-DOPA treatment unless animals became dyskinetic. In L-DOPA-treated animals that developed dyskinesias the level of AT_2R-CB_1R complexes was similar to that found in the striatum of lesioned rats.

3. Discussion

More than one decade ago the interaction between the CB_1R and one angiotensin II receptor, the AT_1, was discovered. Heteromerization was relevant in the periphery, specifically the expression of the CB_1R and AT_1 receptor complex increased in rat hepatic stellate cells upon ethanol administration (Rozenfeld et al., 2011). As earlier described, the CB_1R is the most-expressed GPCR in the mammalian brain where members of the RAS system are also expressed and i) take part in higher functions and ii) are involved in pathophysiological mechanisms of a variety of diseases affecting the CNS. Of particular relevance is the AT_2R function as it seemingly mediates the neuroprotective mechanisms of angiotensin II.

GPCR heteromerization leads to versatility in signaling because provides cell responses that could not be afforded by individual receptors (Agnati et al., 2003; Ferré et al., 2009; Franco et al., 2016). The receptors that have been considered in this manuscript are relevant for fine-tuning motor control and for modulating other higher functions controlled by basal ganglia structures and circuits. On the one hand, the CB_1R interacts to form heteromers with the CB_2R and also with other receptors that are modulated by cannabinoids, e.g. GPR55 and GPR18 (Callén et al., 2012; Lanciego et al., 2011; Martínez-Pilla et al., 2020; Reyes-Resina et al., 2018). These receptors are considered as potential targets in the therapy of Parkinson's and or Huntington's diseases (de

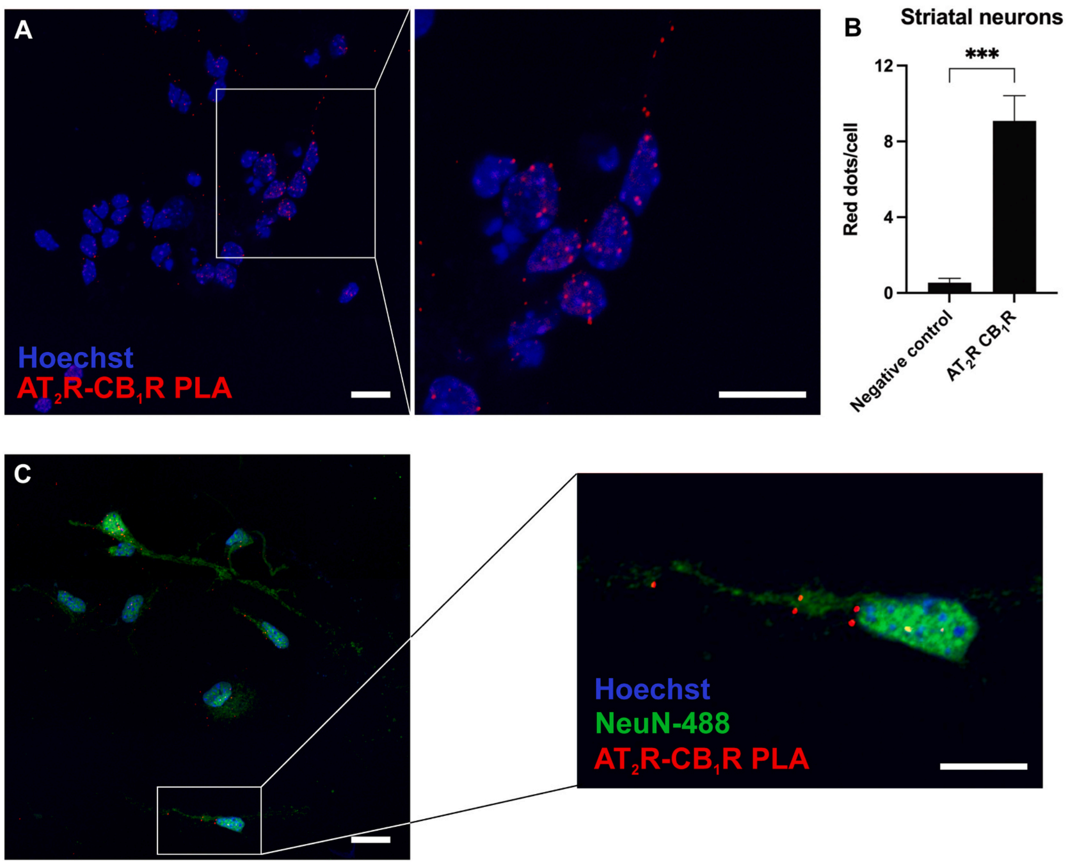

Fig. 5. In situ Proximity Ligation Assay (PLA) performed in primary striatal neurons. PLA assays were performed in primary neurons using specific primary antibodies against AT_2R and against CB_1R (1/100) (see Methods). Representative images corresponding to stacks of 4 sequential planes are shown. Cell nuclei were stained with Hoechst (blue); receptor complexes appear as red dots (Panel A). The number of red dots/cell (bars graph, Panel B) was quantified using the Andy's algorithm Fiji's plug-in (see Methods). The "negative control" represents the condition in which a primary antibody was omitted. In Panel C, an Alexa Fluor®488 conjugated anti-NeuN antibody was used to confirm that red dots were present in neurons. Scale bar: 15 μm. Values are the mean ± S.E.M. of 5 different experiments performed in duplicates. Student's unpaired *t*-test two tailed parametric versus the negative control condition (***$p < 0.001$). (For interpretation of the references to colour in this figure legend, the reader is referred to the web version of this article.)

Lago and Fernández-Ruiz, 2007; Fernández-Ruiz et al., 2015b; Fernández-Ruiz et al., 2015a; Fraguas-Sánchez and Torres-Suárez, 2018; Glass, 2001; Janero, 2012; Maccarrone et al., 2017; Pérez-Olives et al., 2021; Ruiz-Calvo et al., 2019; Velayudhan et al., 2014; Zeissler et al., 2016). On the other hand, the AT_1 and AT_2 angiotensin receptors interact with each other, and may interact with other proteins of the renin-angiotensin RAS system and, among other GPCRs, with adrenergic and bradykinin receptors (Barki-Harrington et al., 2003; Cerrato et al., 2016; Garcia-Garrote et al., 2019; González-Hernández et al., 2010; Rivas-Santisteban et al., 2020; Rozenfeld et al., 2011; Uberti et al., 2003). Antagonists of the AT_1R ("*sartans*") used in the therapy of hypertension, particularly those crossing blood-brain barrier, have been proposed for the therapy of neurodegenerative diseases (Drews et al., 2021; Jo et al., 2022; Kehoe et al., 2021; Lin et al., 2022; Yang et al., 2022) and there are three registered clinical trials using drug combinations including losartan for dementia (Losartan, 2022). Although the AT_2R has been less studied in the CNS, it is expressed in the basal ganglia, and in particular, in striatal neurons. In addition, compensatory mechanisms upon aging and upon neurological alterations include overexpression of the AT_2R in the neurons of some specific CNS areas (Rodriguez-Perez et al., 2020; Villar-Cheda et al., 2014). Consistent with this, recent preclinical studies are exploring the use of AT_2R-centered therapies to combat brain diseases (Ahmed et al., 2022; Royea et al., 2020). In this complex scenario we aimed at assessing whether the cannabinoid CB_1R could interact with angiotensin AT_2 receptors in a heterologous system, in primary striatal neurons and in striatal sections of the 6-OHDA hemilesioned rat model of PD.

Dyskinesias appearing in patients after chronic administration of L-DOPA is a well-known side effect of the medication. Reasons explaining why dyskinesias appear in some patients and not in others and/or why they appear sooner in some patients than in others are unknown (Cesaroni et al., 2022; Kwon et al., 2022; Zhou et al., 2022). It is even more intriguing why rats with the same genetic background and subjected to the same manipulations that end up in PD-like symptoms, behave differently upon chronic L-DOPA administration. Among the few hints about differences between dyskinetic and non-dyskinetic L-DOPA-administered rats is the differential expression of some GPCR heteromers. We here report the upregulation of the AT_2R-CB_1R heteromer in the lesioned striatum and in the striatum of animals that become dyskinetic; in contrast the expression level of animals that respond to L-DOPA treatment and do not become dyskinetic is similar to that in the non-lesioned (control) striatum (Fig. 7). We have reported that L-DOPA disrupts some of the GPCR receptors complexes that are expressed in the non-lesioned rat brain. In fact, the drug alters the formation of the macromolecular complexes formed by three GPCRs; the CB_1R, the adenosine A_{2A} and the dopamine D_2, which are relevant for striatal function (Pinna et al., 2014). L-DOPA disruption of GPCR heteromers has been also detected in the 1-methyl-4-phenyl-1,2,3,6-tetrahydropyridine (MTP) primate model of parkinsonism (Bonaventura et al., 2014). Also in the MPTP primate model, L-DOPA-induced dyskinesia results in the reduction of CB_1-CB_2 receptor heteromers in the basal ganglia outputs neurons. In this specific case the reduction in heteomer expression

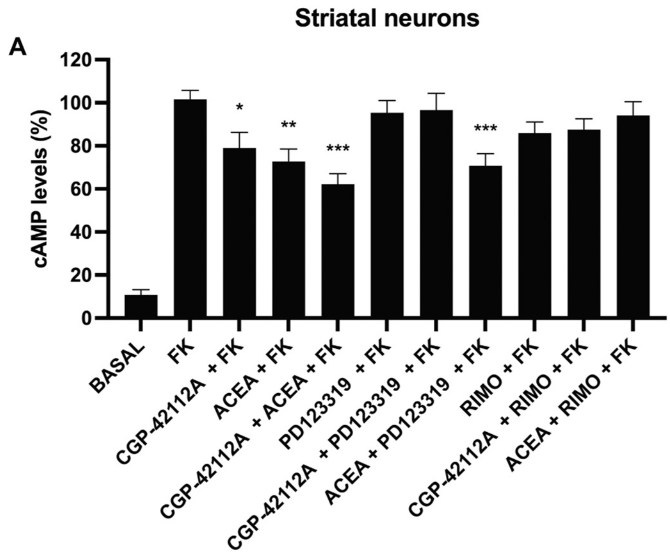

Fig. 6. cAMP determination in primary striatal neurons. Neurons were pretreated for 15 min with vehicle or selective antagonists: PD123319 for the AT_2R or rimonabant (RIMO) for the CB_1R. Then, cells were treated for 15 min with vehicle or agonists: CGP-42112A for AT_2R, ACEA for CB_1R or both. Cells were treated for an additional 15 min with 0.5 μM FK. cAMP levels were determined as described in methods. Values are the mean ± S.E.M. of 5 different experiments performed in triplicates. Values are expressed as percentage of cAMP accumulation induced by forskolin (FK) ($n = 5$, in triplicates). One-way ANOVA followed by Bonferroni's multiple comparison tests were used for statistical analysis. $^{*}p < 0.05$; $^{**}p < 0.01$; $^{***}p < 0.001$, versus FK treatment.

is likely a consequence of reduced expression of the mRNA for both cannabinoid receptors (Sierra et al., 2015).While the real impact of altered GPCR heteromer expression is not known, it should be noted that PD correlates with altered expression of heteromers, with potential rearrangement of receptor complexes, and that L-DOPA treatment introduces further changes in heteromer expression. Whether differential expression of GPCR heteromers in dyskinesias is cause, consequence or epiphenomenon resulting from L-DOPA administration deserves further investigation.

This paper reports the interaction of the CB_1R and the AT_2R in both a heterologous expression system and in striatal neurons. The pharmacological imprint of the heteromer can be disclosed by the use of antagonists of the CB_1R that block AT_2R-mediated Gi-signaling. This imprint was found using two different and selective CB_1R antagonists and served, together with PLA assays, to detect the heteromer in striatal neurons. One of the two antagonists used in the present study, rimonabant, was approved by the FDA to combat obesity, but was withdrawn in 2008 due to serious CNS-related side effects (Sam et al., 2011; Simon and Cota, 2017). The entire field of CB_1R-focused drug discovery is interested on optimizing receptor targeting in terms of finding the most suitable disease, the most suitable drug, the most suitable dose, all combined with few side effects. Our results indicate that CB_1R antagonists would prevent G_i-signaling when striatal AT_2R receptors are activated. Therefore, any therapeutic development focused on the CB_1R should consider that the cannabinoid receptor can interact in basal ganglia neurons with the AT_2R, whose activation correlates with the stimulation of mechanisms that prevent addictive behaviors (Nakaoka et al., 2015) and possibly neurodegenerative/neuroinflammatory diseases (see above).

In summary, we here provide evidence of formation of the cannabinoid CB_1 and angiotensin AT_2 receptor heteromers, whose imprint is observed in primary striatal cultures. The main functional consequence of the interaction between the two receptors is the blockade of AT_2R-mediated G_i-signaling by CB_1R antagonists. There is an upregulation of the expression of the heteromer in the striatum of a rat PD model. Expression of the heteromer returned to normal after L-DOPA treatment unless the animals became dyskinetic after chronic L-DOPA treatment. The heteromer level increase in the striatum of L-DOPA/dyskinetic animals was similar to that in the striatum of lesioned animals before being treated with L-DOPA.

4. Materials and methods

4.1. Reagents

Forskolin (FK), arachidonyl-2′-chloroethylamide (ACEA), CGP-42112A, PD123319, Rimonabant-SR141716 (RIMO), CP-945,598, PolyEthylenImine, 6-hydroxydopamine (6-OHDA) and Hoechst were purchased from Sigma_Aldrich (St Louis, MO, USA). Concentrated (10 mM) stock solutions of agonists/antagonists prepared in ethanol (ACEA), DMSO (RIMO and CP-945,598) or water (CGP-42112A and PD123319) were stored at −20 °C; they were thawed and diluted in vehicle before use.

4.2. Cells

Primary striatal neurons were obtained from 19-day mouse embryos as described in (Hradsky et al., 2013) (Franco et al., 2018). Cells were isolated as described in (Hradsky et al., 2013) and plated at a confluence of 40,000 cells/0.32 cm^2. Briefly, striata were dissected and digested in 0.25% trypsin for 15 min at 37 °C. Trypsinization was stopped by repeated washes with Hank's Buffered Saline Solution (HBSS, Gibco). Cells were brought to a single cell suspension by repeated pipetting followed by passage through a 100 μm-pore mesh. Cells were then resuspended in supplemented DMEM and seeded at a density of 3.5×10^5 cells/mL in six-well plates or 96-well plates for functional assays and in twelve-well plates for immunocytochemistry or PLA assays. The day after, medium was replaced by neurobasal medium supplemented with 2 mM L-glutamine, 100 U/mL penicillin/streptomycin, and 2% (*v*/v) B27 (Gibco) and culture was maintained for 12 days. Cultures were maintained at 37 °C in a 5% CO_2 humid atmosphere. Immunodetection of specific NeuN marker showed that preparations contained >98% neurons.

HEK-293 T cells, batch 70022180, were acquired from the American Type Culture Collection (ATCC). Cells were amplified and frozen in liquid nitrogen in several aliquots. Cells from each aliquot were used until passage 18. HEK-293 T cells were grown in Dulbecco's modified Eagle's medium (DMEM) (Gibco, Paisley, Scotland, UK) supplemented with 2 mM L-glutamine, 100 μg/mL sodium pyruvate, 100 U/mL penicillin/streptomycin, MEM non-essential amino acids solution (1/100) and 5% (*v*/v) heat-inactivated fetal bovine serum (FBS) (all supplements were from Invitrogen, Paisley, Scotland, UK) and maintained at 37 °C in a humid atmosphere of 5% CO_2.

4.3. Cell transfection

HEK-293 T cells were transiently transfected with the corresponding cDNA(s) by the PEI (PolyEthylenImine) method. Briefly, cDNA diluted in 150 mM NaCl was mixed (10 min) with PEI (5.5 mM in nitrogen residues) also prepared in 150 mM NaCl for 10 min. The cDNA-PEI complexes were placed in contact with HEK-293 T cells and were incubated for 4 h in a serum-starved medium. Then, the medium was replaced by a fresh supplemented culture medium and cells were maintained at 37 °C in a 5% CO_2 humid atmosphere. 48 h after transfection, cells were washed, detached, and resuspended in the assay buffer.

4.4. Plasmids

pcDNA3.1-based plasmids encoding for CB_1R or for CB_1R-YFP, AT_2R-Rluc and Sigma1 receptor-YFP fusion proteins were available in our

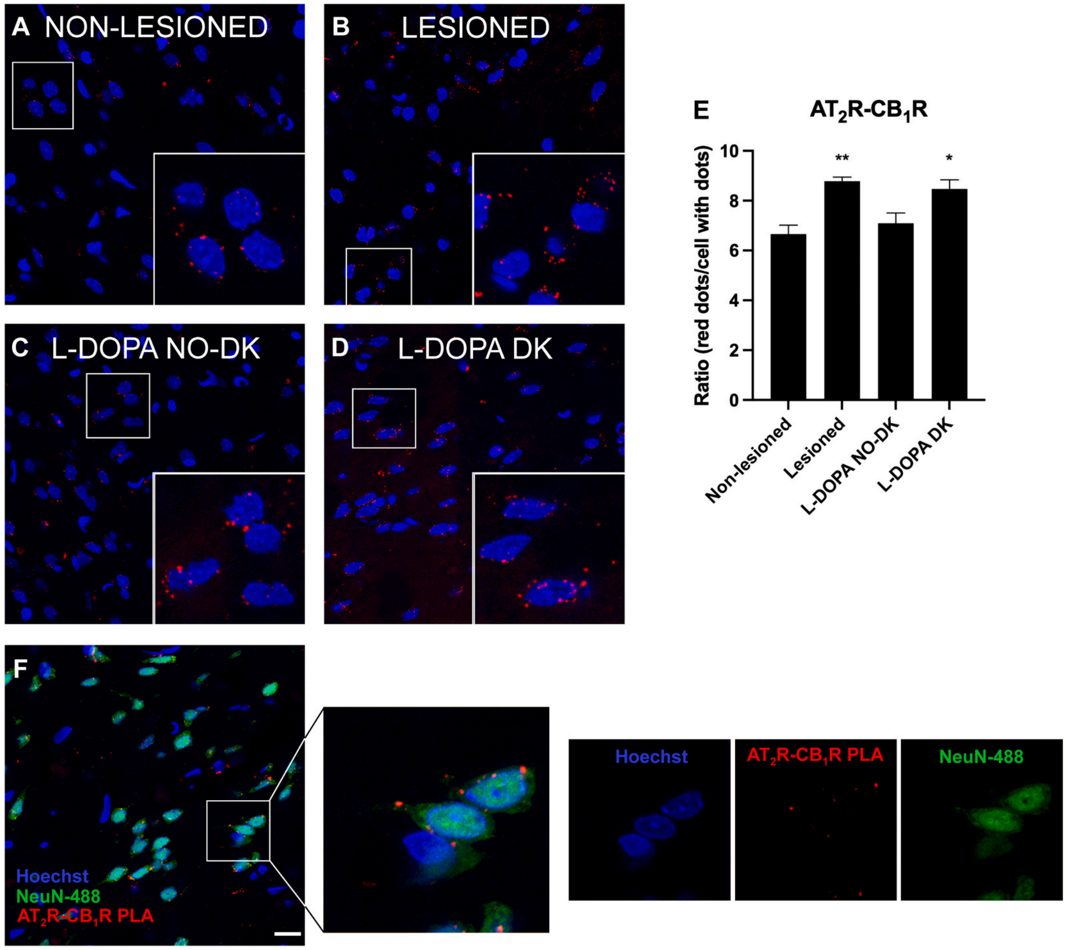

Fig. 7. In situ Proximity Ligation assay (PLA) performed in brain striatal sections of the of 6-OHDA-lesioned rat model. PLA assays were performed in brain striatal sections of four different groups of animals: non-lesioned (A), lesioned (B), lesioned treated with L-DOPA non-dyskinetic (C) and lesioned treated with L-DOPA and dyskinetic (D) using specific primary antibodies against AT_2R and against CB_1R (1/100, each). Representative images corresponding to stacks of 4 sequential planes are shown. Cell nuclei were stained with Hoechst (blue); receptor complexes appear as red dots. The number of red dots/cell with dots (E) was quantified using the Andy's algorithm Fiji's plug-in. Image in panel F was obtained using an Alexa Fluor®488 conjugated anti-NeuN antibody, to confirm that red dots were present in neurons. Scale bar: 15 μm. Values are the mean ± S.E.M. of 5 different experiments performed in triplicates. Student's unpaired *t*-test two tailed parametric versus "non-lesioned" ($^*p < 0.1$ and $^{**}p < 0.01$). (For interpretation of the references to colour in this figure legend, the reader is referred to the web version of this article.)

laboratory. Plasmids encoding fusion proteins were generated by subcloning the coding region of each receptor to be in-frame with restriction sites of pRluc-N1 (Clontech, Heidelberg, Germany) and pEYFP-N1 (PerkinElmer, Wellesley, MA) vectors to provide plasmids that express the receptors with Rluc or YFP proteins fused on the C-terminal end.

4.5. PD model generation, levodopa treatment, and dyskinesia assessment

All experiments were carried out in accordance with EU directives (2010/63/EU and 86/609/CEE) and were approved by the Ethical committee of the University of Santiago de Compostela. Similar to the approach elsewhere described (Lopez-Lopez et al., 2020), our experimental design using male Wistar rats aimed to obtain four groups of animals as described below. Animals were 8 weeks old at the beginning of the experimental procedure.

Details of model generation and the protocol of drug administration and behavioral analysis, performed by a blinded investigator, are given elsewhere (Muñoz et al., 2014). Surgery was performed on rats anesthetized with ketamine/xylazine (1% ketamine, 75 mg/kg, and 2% xylazine, 10 mg/kg). Lesions were produced in the right medial forebrain bundle to achieve a complete degeneration of the nigrostriatal pathway. The rats were injected with 12 μg of 6-hydroxydopamine (6-OHDA) (to provide 8 μg of 6-OHDA hydroxydopamine free base) in 4 μL of sterile saline containing 0.2% ascorbic acid. Animals adequately lesioned were selected ($n = 18$) by rotational behavior (see below). Injection of vehicle led to the generation of naïve (or non-lesioned) animals ($n = 6$).

To identify rats with 6-OHDA-induced maximal dopaminergic lesions, amphetamine-induced rotation was tested in a bank of 8 automated rotometer bowls (Rota-count 8, Columbus Instruments, Columbus, OH, USA) by monitoring full (360°) body turns in either direction. Right and left full body turns were recorded over 90 min following an injection of d-amphetamine (2.5 mg/kg i.p.) dissolved in saline. Rats that displayed more than 6 full body turns/min ipsilateral to the lesion were included in the study (this rate would correspond to >90% depletion of dopamine fibers in the striatum (Winkler et al., 2002). Dopaminergic lesions were confirmed with the cylinder test. Spontaneous use of forelimb was measured by the cylinder test (Kirik et al., 2001). Rats were placed individually in a glass cylinder (20 cm in diameter) and the number of left or right forepaw contacts was scored by an observer blinded to the animals' identity and presented as left (impaired) touches as a percentage of total touches. A control animal would thus receive an unbiased score of 50%, whereas the lesion usually reduces the performance of the impaired paw to less than 20% of total wall contacts.

Of the lesioned animals selected according to the above-described tests (18 in total), 12 were chronically treated with L-DOPA daily for 3 weeks, 6 with vehicle instead L-DOPA. A mixture of L-DOPA methyl ester (6 mg/kg) plus benserazide (10 mg/kg) was administered subcutaneously. The treatment reliably induces dyskinetic movements in some rats. Abnormal involuntary movements were evaluated according to the rat dyskinesia scale described in a previous report (Farré et al., 2015). The severity of each abnormal involuntary movement (AIM) subtype (limb, orolingual, and axial) was assessed using scores from 0 to 4 (1 = occasional, present $< 50\%$ of the time; 2 = frequent, present $> 50\%$ of the time; 3 = continuous but interrupted by strong sensory stimuli; 4 = continuous, not interrupted by strong sensory stimuli). Rats were classified as "dyskinetic" if they displayed a score ≥ 2 per monitoring period on at least two AIM subtypes. Animals classified as "non-dyskinetic" exhibited either no L-DOPA-induced abnormal involuntary movements or very mild/occasional ones. Animals with low scores, either non-dyskinetic or dyskinetic, were excluded. In summary, four groups of animals were obtained: [1] non-lesioned [2] lesioned, treated with vehicle; [3] lesioned and became dyskinetic when treated with L-DOPA; and [4] lesioned and did not become dyskinetic upon L-DOPA treatment. Tyrosine hydroxylase immunostaining was performed in every animal from sections taken postmortem; selected animals undergoing 6-OHDA treatment showed, in the lesioned hemisphere, $>95\%$ nigral dopaminergic denervation. Overall, 4 animals (those with better scores) were selected in each of the following 4 groups: naïve, lesioned, lesioned/L-DOPA dyskinetic, and lesioned/L-DOPA non-dyskinetic. The PLA analysis (see below) was performed in different fields of striatal sections from each of the 16 selected animals. The striatum was delimited in sections using a bright field, and images were captured within delimitation coordinates.

4.6. Immunocytochemistry

HEK-293 T cells were seeded on glass coverslips in 12-well plates. Twenty-four hours later, cells were transfected with cDNA for CB_1R-YFP cDNA, with cDNA for CB_1R and/or with cDNA for AT_2R-Rluc. Forty-eight hours after transfection, cells were fixed in 4% paraformaldehyde for 15 min and washed twice with PBS containing 20 mM glycine before permeabilization with PBS-glycine containing 0.2% Triton X-100 (5 min incubation). Blocking was performed with PBS containing 1% bovine serum albumin (1 h). Then cells were incubated (1 h) with a mouse anti-Rluc antibody (1/100, MAB4400, Millipore, Merck, Darmstadt, Germany) and subsequently incubated (1 h) with a sulfo-cyanine3 (Cy3)-conjugated anti-mouse IgG secondary antibody (1/200, 715–166-150 (red), Jackson ImmunoResearch, St. Thomas Place, UK). CB_1R-YFP expression was detected by the YFP's own fluorescence. CB_1R expression was detected by labeling with a rabbit anti-CB_1R antibody (1:100, ThermoFisher ref.: Catalog #PA1–745) and a secondary Alexa Fluor®488 conjugated anti-rabbit antibody (1:200, ThermoFisher Ref: A-11008). Nuclei were stained with Hoechst (1/100 from stock 1 mg/mL). Samples were washed several times and mounted with Immu-mount® (FisherScientific). Images were obtained in a Zeiss LSM 880 confocal microscope (ZEISS, Germany) using the 63× oil objective.

4.7. Bioluminescence resonance energy transfer (BRET) assays

HEK-293 T cells were transiently cotransfected with a constant amount of cDNA encoding for AT_2-Rluc (1 μg) and with increasing amounts of cDNA corresponding to either CB_1R-YFP (0.4 to 1.6 μg) or with σ_1R-YFP (0.25 to 2.5 μg), as a negative control for BRET assay. To assess cell amount, protein concentration was determined using a Bradford assay kit (Bio-Rad, Munich, Germany) using bovine serum albumin (BSA) dilutions as standards. To quantify fluorescent proteins, cells (20 μg total protein) were distributed in 96-well microplates (black plates with a transparent bottom) and fluorescence was read in a Fluostar Optima Fluorimeter (BMG Labtech, Offenburg, Germany) equipped with a high-energy xenon flash lamp, using a 10-nm bandwidth excitation filter at 485 nm. For BRET measurements, the equivalent of 20 μg protein cell suspension was distributed in 96-well white microplates with a white bottom (Corning 3600, Corning, NY). For BRET measurements, the equivalent to 20 μg protein cell suspension was distributed in 96-well microplates (white plates, Porvair, Leatherhead, UK) and 5 μM coelenterazine H was added (PJK GMBH, Kleinblittersdorf, Germany). One min after coelenterazine H addition, the readings were collected using a Mithras LB 940 (Berthold, Bad Wildbad, Germany), which allowed the integration of the signals detected in the short-wavelength filter at 485 nm (440–500 nm) and the long-wavelength filter at 530 nm (510–590 nm). To quantify receptor-Rluc expression, luminescence readings were collected 10 min after addition of 5 μM coelenterazine H. The net BRET is defined as [(long-wavelength emission)/(short-wavelength emission)]-Cf, where Cf corresponds to [(long-wavelength emission)/(short-wavelength emission)] for the Rluc construct expressed alone in the same experiment. Data in BRET curves that depict an equilateral hyperbola were fitted using an only tool (Herraez, 2022). MilliBRET units (mBU) are defined as:

$$\mathrm{mBU} = \left[\frac{\lambda_{530}(\mathrm{long} - \mathrm{wavelength\ emission})}{\lambda_{485}(\mathrm{short} - \mathrm{wavelength\ emission})} - \mathrm{C_f} \right] x\ 1000$$

where C_f corresponds to [(long-wavelength emission)/(short-wavelength emission)] for the Rluc construct expressed alone in the same experiment.

4.8. cAMP level determination

Determination of intracellular cAMP levels was performed in HEK-293 T cells transfected with the cDNA for AT_2R (1.5 μg), the cDNA for the CB_1R (1.5 μg) or both. Two hours before the experiment, the medium was replaced by serum-starved DMEM medium. HEK-293 T cells (≈2000 by well) growing in a medium containing 50 μM zardaverine were distributed in 384-well microplates and treated with vehicle or with a selective AT_2R antagonist (PD123319, 1 μM) or with selective CB_1R antagonists (Rimonabant, 1 μM or CP-945,598, 1 μM). 15 min later, cells were treated with the AT_2R agonist (CGP-42112A, 100 nM) and/or the CB_1R agonist (ACEA, 100 nM) for 15 min before adding 0.5 μM FK or vehicle for an additional 15 min period. The Lance Ultra cAMP kit (PerkinElmer, ref. TRF0262) was used prior homogeneous time-resolved fluorescence energy transfer (HTRF) measurements. HTRF (665 nm) was determined on a PHERAstar Flagship microplate reader equipped with an HTRF optical module (BMG Labtech). A standard curve for cAMP was obtained in each experiment.

4.9. β-arrestin II recruitment assays

HEK-293 T cells were transiently transfected as described in *Cell transfection* with 0.4 μg of cDNA coding for β-arrestin II-Rluc and 1.5 μg of cDNAs coding for AT_2R-YFP and/or CB_1R-YFP. 48 h later, cells were treated for 5 min with vehicle (control) or with the AT_2R and/or CB_1R agonists (100 nM CGP-42112A and/or 100 nM ACEA). Then, cells were fixed with paraformaldehyde (4%) and subsequently processed as in *Immunocytochemistry.* ß-arrestin II recruitment was analyzed by determining the colocalization of the fluorescence signal between the YFP-labeled receptor and ß-arrestin II-Rluc labeled with an anti-Rluc primary antibody and a Cy3-conjugated secondary antibody. To measure the degree of correlation (linear) between the red (ß-arrestin II) and the green (receptor) channels, the Pearson's correlation coefficient was calculated with Fiji software (Analyze > Coloc2 plugin) using the images obtained in the confocal microscope.

4.10. In situ Proximity Ligation Assay (PLA)

Occurrence of AT_2R and CB_1R heteromers in primary neurons and in brain sections was detected using the Duolink in situ PLA detection Kit (OLink; Bioscience, Uppsala, Sweden ref. DUO92008) following the instructions of the supplier. Primary neurons were grown on glass coverslips, fixed in 4% paraformaldehyde for 15 min, washed with PBS containing 20 mM glycine to quench the aldehyde groups and permeabilized with the same buffer containing 0.05% Triton X-100 (20 min). Then, samples were washed with PBS and incubated (1 h) at 37 °C with blocking solution (Sigma_Aldrich, ref. DUO82007) in a pre-heated humidity chamber. After overnight incubation with the antibody diluent medium having a mixture of equal amounts of rabbit anti-AT_2R (ab92445, Abcam) (1/100) and mouse anti-CB_1R (sc-518,035, Santa-Cruz) antibodies (1/100), ligation and amplification were conducted as indicated by the supplier. Neurons were identified by staining with the Alexa Fluor®488 conjugated anti-NeuN antibody (ab190195). Samples were mounted using the mounting medium with Hoechst (1/100) to stain nuclei. Samples were observed in a Zeiss 880 confocal microscope (Carl Zeiss, Oberkochen, Germany) equipped with an apochromatic 63× oil immersion objective (N.A. 1.4) and 405 nm, 488 nm and 561 nm laser lines. For each field of view, a stack of two channels (one per staining) and four Z stacks with a step size of 1 μm were acquired. The number of neurons containing one or more red spots versus total cells (blue nucleus) was determined, and Student's *t*-test was used to compare the values (red dots/cell).

4.11. Statistical analysis

GraphPad Prism 9.4 software (San Diego, CA, USA) was used for data analysis. One-way ANOVA followed by post hoc Bonferroni's test, post hoc Tukey's test or Dunnett's test were used when multiple comparison analysis. BRET parameters were calculated using an ad hoc on-line tool (Herraez, 2022). In PLA assays the number of red dots/cell was determined using the Andy's algorithm Fiji's plug-in (Law et al., 2017). Two-tailed Student's *t*-test was used for PLA statistical analysis.

Ethical approval

Animal handling, sacrifice, and further experiments were conducted according to the guidelines set in Directive 2010/63/EU of the European Parliament and the Council of the European Union that is enforced in Spain by National and Regional organisms; the 3R rule (replace, refine, reduce) for animal experimentation was also taken into account. By the current legislation, protocol approval is not needed if animals are sacrificed to obtain a specific tissue.

Author contributions

RF, GN and JLLG designed the project and protocols to perform assays using brain tissue from an animal model of Parkinson's disease. RRS performed experiments in the heterologous system and signaling assays in striatal neurons. JL, IR and AL did brain dissection and prepared primary striatal neurons. AM and AIRP did animal lesioning and obtained brain sections for PLA analysis; they also prepared the final PLA images in Figs. 4, 5 and 7. RF and RRS wrote the first draft. All authors have edited the manuscript and have approved the submitted version.

Funding

This work was supported by grants PID2020-113430RB-I00 and PID2021-126600OB-I00 funded by Spanish MCIN/AEI/10.13039/501100011033 and, as appropriate, by "ERDF A way of making Europe", by the "European Union" or by the "European Union Next Generation EU/PRTR". The research group of the University of Barcelona is considered of excellence (grup consolidat #2017 SGR 1497) by the Regional Catalonian Government, which does not provide any specific funding for reagents or for payment of services or Open Access fees.

Declaration of Competing Interest

Authors declare neither conflict of interest nor competing interests.

Data availability

Data will be made available on request.

Appendix A. Supplementary data

Supplementary data to this article can be found online at https://doi.org/10.1016/j.expneurol.2023.114319.

References

Agnati, L.F., Franzen, O., Ferre, S., Leo, G., Franco, R., Fuxe, K., 2003. Possible role of intramembrane receptor-receptor interactions in memory and learning via formation of long-lived heteromeric complexes: focus on motor learning in the basal ganglia. J. Neural Transm. Suppl. 1–28.

Ahmed, H.A., Ismael, S., Salman, M., Devlin, P., McDonald, M.P., Liao, F.F., Ishrat, T., 2022. Direct AT2R Stimulation Slows Post-stroke Cognitive Decline in the 5XFAD Alzheimer's Disease Mice. Mol. Neurobiol. 59, 4124–4140. https://doi.org/10.1007/S12035-022-02839-X.

Alexander, S.P., Christopoulos, A., Davenport, A.P., Kelly, E., Mathie, A., Peters, J.A., Veale, E.L., Armstrong, J.F., Faccenda, E., Harding, S.D., Pawson, A.J., Southan, C., Davies, J.A., Abbracchio, M.P., Alexander, W., Al-hosaini, K., Bäck, M., Barnes, N.M., Bathgate, R., Beaulieu, J.-M., Bernstein, K.E., Bettler, B., Birdsall, N.J.M., Blaho, V., Boulay, F., Bousquet, C., Bräuner-Osborne, H., Burnstock, G., Caló, G., Castaño, J.P., Catt, K.J., Ceruti, S., Chazot, P., Chiang, N., Chini, B., Chun, J., Cianciulli, A., Civelli, O., Clapp, L.H., Couture, R., Csaba, Z., Dahlgren, C., Dent, G., Singh, K.D., Douglas, S.D., Dournaud, P., Eguchi, S., Escher, E., Filardo, E.J., Fong, T., Fumagalli, M., Gainetdinov, R.R., Gasparo, M. de, Gerard, C., Gershengorn, M., Gobeil, F., Goodfriend, T.L., Goudet, C., Gregory, K.J., Gundlach, A.L., Hamann, J., Hanson, J., Hauger, R.L., Hay, D.L., Heinemann, A., Hollenberg, M.D., Holliday, N. D., Horiuchi, M., Hoyer, D., Hunyady, L., Husain, A., IJzerman, A.P., Inagami, T., Jacobson, K.A., Jensen, R.T., Jockers, R., Jonnalagadda, D., Karnik, S., Kaupmann, K., Kemp, J., Kennedy, C., Kihara, Y., Kitazawa, T., Kozielewicz, P., Kreienkamp, H.-J., Kukkonen, J.P., Langenhan, T., Leach, K., Lecca, D., Lee, J.D., Leeman, S.E., Leprince, J., Li, X.X., Williams, T.L., Lolait, S.J., Lupp, A., Macrae, R., Maguire, J., Mazella, J., McArdle, C.A., Melmed, S., Michel, M.C., Miller, L.J., Mitolo, V., Mouillac, B., Müller, C.E., Murphy, P., Nahon, J.-L., Ngo, T., Norel, X., Nyimanu, D., O'Carroll, A.-M., Offermanns, S., Panaro, M.A., Parmentier, M., Pertwee, R.G., Pin, J.-P., Prossnitz, E.R., Quinn, M., Ramachandran, R., Ray, M., Reinscheid, R.K., Rondard, P., Rovati, G.E., Ruzza, C., Sanger, G.J., Schöneberg, T., Schulte, G., Schulz, S., Segaloff, D.L., Serhan, C.N., Stoddart, L.A., Sugimoto, Y., Summers, R., Tan, V.P., Thal, D., Thomas, W. (Wally), Timmermans, P.B.M.W.M., Tirupula, K., Tulipano, G., Unal, H., Unger, T., Valant, C., Vanderheyden, P., Vaudry, D., Vaudry, H., Vilardaga, J.-P., Walker, C.S., Wang, J.M., Ward, D.T., Wester, H.-J., Willars, G.B., Woodruff, T.M., Yao, C., Ye, R.D., 2021. The concise guide to pharmacology 2021/22: G protein-coupled receptors. Br. J. Pharmacol. 178, S27–S156. https://doi.org/10.1111/BPH.15538.

Barki-Harrington, L., Luttrell, L.M., Rockman, H.A., 2003. Dual Inhibition of β-Adrenergic and Angiotensin II Receptors by a Single Antagonist. Circulation 108, 1611–1618. https://doi.org/10.1161/01.CIR.0000092166.30360.78.

Barnes, J.M., Steward, L.J., Barber, P.C., Barnes, N.M., 1993. Identification and characterisation of angiotensin II receptor subtypes in human brain. Eur. J. Pharmacol. 230, 251–258. https://doi.org/10.1016/0014-2999(93)90558-Y.

Basavarajappa, B.S., Shivakumar, M., Joshi, V., Subbanna, S., 2017. Endocannabinoid system in neurodegenerative disorders. J. Neurochem. 142, 624–648. https://doi.org/10.1111/jnc.14098.

Bonaventura, J., Rico, A.J., Moreno, E., Sierra, S., Sánchez, M., Luquin, N., Farré, D., Müller, C.E., Martínez-Pinilla, E., Cortés, A., Mallol, J., Armentero, M.-T., Pinna, A., Canela, E.I., Lluís, C., McCormick, P.J., Lanciego, J.L., Casadó, V., Franco, R., 2014. L-DOPA-treatment in primates disrupts the expression of A(2A) adenosine-CB(1) cannabinoid-D(2) dopamine receptor heteromers in the caudate nucleus. Neuropharmacology 79, 90–100. https://doi.org/10.1016/j.neuropharm.2013.10.036.

Callén, L., Moreno, E., Barroso-Chinea, P., Moreno-Delgado, D., Cortés, A., Mallol, J., Casadó, V., Lanciego, J.L., Franco, R., Lluis, C., Canela, E.I., McCormick, P.J., 2012. Cannabinoid receptors CB1 and CB2 form functional heteromers in brain. J. Biol. Chem. 287, 20851–20865. https://doi.org/10.1074/jbc.M111.335273.

Castillo, A., Tolón, M.R., Fernández-Ruiz, J., Romero, J., Martinez-Orgado, J., 2010. The neuroprotective effect of cannabidiol in an in vitro model of newborn hypoxic-ischemic brain damage in mice is mediated by CB2and adenosine receptors. Neurobiol. Dis. 37, 434–440. https://doi.org/10.1016/j.nbd.2009.10.023.

Cerrato, B.D., Carretero, O.A., Janic, B., Grecco, H.E., Gironacci, M.M., 2016. Heteromerization Between the Bradykinin B2 Receptor and the Angiotensin-(1-7) Mas Receptor: Functional Consequences. Hypertens. (Dallas, Tex. 1979) 68, 1039–1048. https://doi.org/10.1161/HYPERTENSIONAHA.116.07874.

Cesaroni, V., Blandini, F., Cerri, S., 2022. Dyskinesia and Parkinson's disease: animal model, drug targets and agents in preclinical testing. Expert Opin. Ther. Targets. https://doi.org/10.1080/14728222.2022.2153036.

Conlin, P.R., 2000. Angiotensin II Antagonists in the Treatment of Hypertension: More Similarities Than Differences. J. Clin. Hypertens. (Greenwich). 2, 253–257.
Drews, H.J., Klein, R., Lourhmati, A., Buadze, M., Schaeffeler, E., Lang, T., Seferyan, T., Hanson, L.R., Frey, W.H., de Vries, T.C.G.M., Thijssen-Van Loosdregt, I.A.E.W., Gleiter, C.H., Schwab, M., Danielyan, L., 2021. Losartan Improves Memory, Neurogenesis and Cell Motility in Transgenic Alzheimer's Mice. Pharmaceuticals (Basel) 14, 1–17. https://doi.org/10.3390/PH14020166.
Farré, D., Muñoz, A., Moreno, E., Reyes-Resina, I., Canet-Pons, J., Dopeso-Reyes, I.G., Rico, A.J., Lluís, C., Mallol, J., Navarro, G., Canela, E.I., Cortés, A., Labandeira-García, J.L., Casadó, V., Lanciego, J.L., Franco, R., 2015. Stronger Dopamine D1 Receptor-Mediated Neurotransmission in Dyskinesia. Mol. Neurobiol. 52, 1408–1420. https://doi.org/10.1007/s12035-014-8936-x.
Fernández-López, D., Pazos, M.R., Tolón, R.M., Moro, M.A., Romero, J., Lizasoain, I., Martínez-Orgado, J., 2007. The cannabinoid agonist WIN55212 reduces brain damage in an in vivo model of hypoxic-ischemic encephalopathy in newborn rats. Pediatr. Res. 62, 255–260. https://doi.org/10.1203/PDR.0b013e318123fbb8.
Fernández-Ruiz, J., Romero, J., Ramos, J., 2015b. Endocannabinoids and Neurodegenerative Disorders: Parkinson's Disease, Huntington's Chorea, Alzheimer's Disease, and Others. Handb. Exp. Pharmacol. 231, 233–259. https://doi.org/10.1007/978-3-319-20825-1_8.
Fernández-Ruiz, Javier, Moro, M.A., Martínez-Orgado, J., 2015a. Cannabinoids in Neurodegenerative Disorders and Stroke/Brain Trauma: From Preclinical Models to Clinical Applications. Neurotherapeutics 12, 793–806. https://doi.org/10.1007/s13311-015-0381-7.
Ferré, S., Baler, R., Bouvier, M., Caron, M.G., Devi, L.A., Durroux, T., Fuxe, K., George, S. R., Javitch, J.A., Lohse, M.J., Mackie, K., Milligan, G., Pfleger, K.D.G., Pin, J.-P., Volkow, N.D., Waldhoer, M., Woods, A.S., Franco, R., 2009. Building a new conceptual framework for receptor heteromers. Nat. Chem. Biol. 5, 131–134. https://doi.org/10.1038/nchembio0309-131.
Fraguas-Sánchez, A.I., Torres-Suárez, A.I., 2018. Medical Use of Cannabinoids. Drugs 78, 1665–1703. https://doi.org/10.1007/s40265-018-0996-1.
Franco, R., Martínez-Pinilla, E., Lanciego, J.L., Navarro, G., 2016. Basic pharmacological and structural evidence for class A G-protein-coupled receptor heteromerization. Front. Pharmacol. 7, 1–10. https://doi.org/10.3389/fphar.2016.00076.
Franco, R., Aguinaga, D., Reyes, I., Canela, E.I., Lillo, J., Tarutani, A., Hasegawa, M., Del Ser-Badia, A., del Rio, J.A., Kreutz, M.R., Saura, C.A., Navarro, G., 2018. N-Methyl-D-Aspartate Receptor Link to the MAP Kinase Pathway in Cortical and Hippocampal Neurons and Microglia Is Dependent on Calcium Sensors and Is Blocked by α-Synuclein, Tau, and Phospho-Tau in Non-transgenic and Transgenic APPSw. Ind Mice. Front. Mol. Neurosci. 11, 273. https://doi.org/10.3389/fnmol.2018.00273.
Franco, R., Villa, M., Morales, P., Reyes-Resina, I., Gutiérrez-Rodríguez, A., Jiménez, J., Jagerovic, N., Martínez-Orgado, J., Navarro, G., 2019. Increased expression of cannabinoid CB2 and serotonin 5-HT1A heteroreceptor complexes in a model of newborn hypoxic-ischemic brain damage. Neuropharmacology 152, 58–66. https://doi.org/10.1016/j.neuropharm.2019.02.004.
Garcia-Garrote, M., Perez-Villalba, A., Garrido-Gil, P., Belenguer, G., Parga, J.A., Perez-Sanchez, F., Labandeira-Garcia, J.L., Fariñas, I., Rodriguez-Pallares, J., 2019. Interaction between Angiotensin Type 1, Type 2, and Mas Receptors to Regulate Adult Neurogenesis in the Brain Ventricular–Subventricular Zone. Cells 8, 1551. https://doi.org/10.3390/cells8121551.
Garrido-Gil, P., Valenzuela, R., Villar-Cheda, B., Lanciego, J.L., Labandeira-Garcia, J.L., 2013. Expression of angiotensinogen and receptors for angiotensin and prorenin in the monkey and human substantia nigra: an intracellular renin-angiotensin system in the nigra. Brain Struct. Funct. 218, 373–388. https://doi.org/10.1007/s00429-012-0402-9.
Garrido-Gil, P., Rodriguez-Perez, A.I., Fernandez-Rodriguez, P., Lanciego, J.L., Labandeira-Garcia, J.L., 2017. Expression of angiotensinogen and receptors for angiotensin and prorenin in the rat and monkey striatal neurons and glial cells. Brain Struct. Funct. 222, 2559–2571. https://doi.org/10.1007/s00429-016-1357-z.
Garrido-Gil, P., Pedrosa, M.A., Garcia-Garrote, M., Pequeño-Valtierra, A., Rodríguez-Castro, J., García-Souto, D., Rodríguez-Pérez, A.I., Labandeira-Garcia, J.L., 2022. Microglial angiotensin type 2 receptors mediate sex-specific expression of inflammatory cytokines independently of circulating estrogen. Glia 70, 2348–2360. https://doi.org/10.1002/GLIA.24255.
Glass, M., 2001. The role of cannabinoids in neurodegenerative diseases. Prog. Neuro-Psychopharmacology Biol. Psychiatry 25, 743–765. https://doi.org/10.1016/S0278-5846(01)00162-2.
González-Hernández, M.D.L., Godínez-Hernández, D., Bobadilla-Lugo, R.A., López-Sánchez, P., 2010. Angiotensin-II type 1 receptor (AT1R) and alpha-1D adrenoceptor form a heterodimer during pregnancy-induced hypertension. Auton. Autacoid Pharmacol. 30, 167–172. https://doi.org/10.1111/j.1474-8673.2009.00446.x.
Halbach O., Von Bohlen Und, Albrecht, D., 2006. The CNS renin-angiotensin system. Cell Tissue Res. 326, 599–616. https://doi.org/10.1007/S00441-006-0190-8.
Herraez, A., 2022. BRET analysis [WWW Document]. https://biomodel.uah.es/lab/calculos/regresion/BRET.htm (accessed 12.6.22).
Hradsky, J., Mikhaylova, M., Karpova, A., Kreutz, M.R., Zuschratter, W., 2013. Super-resolution microscopy of the neuronal calcium-binding proteins Calneuron-1 and Caldendrin. Methods Mol. Biol. 963, 147–169. https://doi.org/10.1007/978-1-62703-230-8_10.
Jackson, L., Eldahshan, W., Fagan, S.C., Ergul, A., 2018. Within the Brain: The Renin Angiotensin System. Int. J. Mol. Sci. 19 https://doi.org/10.3390/IJMS19030876.
Janero, D.R., 2012. Cannabinoid-1 receptor (CB1R) blockers as medicines: beyond obesity and cardiometabolic disorders to substance abuse/drug addiction with CB1R neutral antagonists. Expert Opin. Emerg. Drugs 17, 17–29. https://doi.org/10.1517/14728214.2012.660916.
Jo, Y., Kim, S., Ye, B.S., Lee, E., Yu, Y.M., 2022. Protective Effect of Renin-Angiotensin System Inhibitors on Parkinson's Disease: A Nationwide Cohort Study. Front. Pharmacol. 13 https://doi.org/10.3389/FPHAR.2022.837890.
Junior, N.C.F., dos-Santos-Pereira, M., Guimarães, F.S., Del Bel, E., 2020. Cannabidiol and Cannabinoid Compounds as Potential Strategies for Treating Parkinson's Disease and L-DOPA-Induced Dyskinesia. Neurotox. Res. 37, 12–29. https://doi.org/10.1007/S12640-019-00109-8.
Kamath, T., Abdulraouf, A., Burris, S.J., Langlieb, J., Gazestani, V., Nadaf, N.M., Balderrama, K., Vanderburg, C., Macosko, E.Z., 2022. Single-cell genomic profiling of human dopamine neurons identifies a population that selectively degenerates in Parkinson's disease. Nat. Neurosci. 25, 588–595. https://doi.org/10.1038/S41593-022-01061-1.
Kehoe, P.G., Turner, N., Howden, B., Jarutyt, L., Clegg, S.L., Malone, I.B., Barnes, J., Nielsen, C., Sudre, C.H., Wilson, A., Thai, N.J., Blair, P.S., Coulthard, E.J., Lane, J.A., Passmore, P., Taylor, J., Mutsaerts, H.-J., Thomas, D.L., Fox, N.C., Wilkinson, I., Ben-Shlomo, Y., 2021. Losartan to slow the progression of mild-to-moderate Alzheimer's disease through angiotensin targeting: the RADAR RCT. Effic. Mech. Eval. 8, 1–72. https://doi.org/10.3310/EME08190.
Kirik, D., Winkler, C., Björklund, A., 2001. Growth and Functional Efficacy of Intrastriatal Nigral Transplants Depend on the Extent of Nigrostriatal Degeneration. J. Neurosci. 21, 2889–2896. https://doi.org/10.1523/JNEUROSCI.21-08-02889.2001.
Kwon, D.K., Kwatra, M., Wang, J., Ko, H.S., 2022. Levodopa-Induced Dyskinesia in Parkinson's Disease: Pathogenesis and Emerging Treatment Strategies. Cells 11, 3736. https://doi.org/10.3390/CELLS11233736.
Labandeira-Garcia, J.L., Parga, J.A., 2022. Nigral Neurons Degenerating in Parkinson's Disease Express the Angiotensin Receptor Type 1 Gene. Mov. Disord. 37, 1610–1611. https://doi.org/10.1002/MDS.29137.
Labandeira-Garcia, J.L., Rodriguez-Pallares, J., Dominguez-Meijide, A., Valenzuela, R., Villar-Cheda, B., Rodríguez-Perez, A.I., 2013. Dopamine-angiotensin interactions in the basal ganglia and their relevance for Parkinson's disease. Mov. Disord. 28, 1337–1342. https://doi.org/10.1002/mds.25614.
Labandeira-Garcia, J.L., Valenzuela, R., Costa-Besada, M.A., Villar-Cheda, B., Rodriguez-Perez, A.I., 2021. The intracellular renin-angiotensin system: Friend or foe. Some light from the dopaminergic neurons. Prog. Neurobiol. 199 https://doi.org/10.1016/J.PNEUROBIO.2020.101919.
de Lago, E., Fernández-Ruiz, J., 2007. Cannabinoids and neuroprotection in motor-related disorders. CNS Neurol. Disord. Drug Targets 6, 377–387. https://doi.org/10.2174/187152707783399210.
Lanciego, J.L., Barroso-Chinea, P., Rico, A.J., Conte-Perales, L., Callén, L., Roda, E., Gómez-Bautista, V., López, I.P., Lluis, C., Labandeira-García, J.L., Franco, R., 2011. Expression of the mRNA coding the cannabinoid receptor 2 in the pallidal complex of *Macaca fascicularis*. J. Psychopharmacol. 25, 97–104. https://doi.org/10.1177/0269881110367732.
Law, A.M.K., Yin, J.X.M., Castillo, L., Young, A.I.J., Piggin, C., Rogers, S., Caldon, C.E., Burgess, A., Millar, E.K.A., O'Toole, S.A., Gallego-Ortega, D., Ormandy, C.J., Oakes, S.R., 2017. Andy's Algorithms: new automated digital image analysis pipelines for FIJI. Sci. Rep. 7, 15717. https://doi.org/10.1038/s41598-017-15885-6.
Lin, H.C., Tseng, Y.F., Shen, A.L., Chao, J.C.J., Hsu, C.Y., Lin, H.L., 2022. Association of Angiotensin Receptor Blockers with Incident Parkinson Disease in Patients with Hypertension: A Retrospective Cohort Study. Am. J. Med. 135, 1001–1007. https://doi.org/10.1016/J.AMJMED.2022.04.029.
Lopez-Lopez, A., Labandeira, C.M., Labandeira-Garcia, J.L., Muñoz, A., 2020. Rho kinase inhibitor fasudil reduces l-DOPA-induced dyskinesia in a rat model of Parkinson's disease. Br. J. Pharmacol. 177, 5622–5641. https://doi.org/10.1111/BPH.15275.
Losartan, C., 2022. Losartan for dementia [WWW Document]. https://clinicaltrials.gov/ct2/results?cond=Alzheimer+Disease&term=losartan&cntry=&state=&city=&dist=&Search=Search (accessed 12.6.22).
Maccarrone, M., Maldonado, R., Casas, M., Henze, T., Centonze, D., 2017. Cannabinoids therapeutic use: what is our current understanding following the introduction of THC, THC:CBD oromucosal spray and others? Expert Rev. Clin. Pharm. 10, 443–455. https://doi.org/10.1080/17512433.2017.1292849.
Martínez-Pinilla, E., Reyes-Resina, I., Oñatibia-Astibia, A., Zamarbide, M., Ricobaraza, A., Navarro, G., Moreno, E., Dopeso-Reyes, I.G.G., Sierra, S., Rico, A.J.J., Roda, E., Lanciego, J.L.L., Franco, R., 2014. CB1 and GPR55 receptors are co-expressed and form heteromers in rat and monkey striatum. Exp. Neurol. 261, 44–52. https://doi.org/10.1016/j.expneurol.2014.06.017.
Martínez-Pinilla, E., Aguinaga, D., Navarro, G., Rico, A.J., Oyarzábal, J., Sánchez-Arias, J.A., Lanciego, J.L., Franco, R., 2019. Targeting CB 1 and GPR55 Endocannabinoid Receptors as a Potential Neuroprotective Approach for Parkinson's Disease. Mol. Neurobiol. 56, 5900–5910. https://doi.org/10.1007/S12035-019-1495-4.
Martínez-Pinilla, E., Rico, A.J., Rivas-Santisteban, R., Lillo, J., Roda, E., Navarro, G., Lanciego, J.L., Franco, R., 2020. Expression of GPR55 and either cannabinoid CB 1 or CB 2 heteroreceptor complexes in the caudate, putamen, and accumbens nuclei of control, parkinsonian, and dyskinetic non-human primates. Brain Struct. Funct. 225, 2153–2164. https://doi.org/10.1007/S00429-020-02116-4.
Muñoz, A., Garrido-Gil, P., Dominguez-Meijide, A., Labandeira-Garcia, J.L., 2014. Angiotensin type 1 receptor blockage reduces l-dopa-induced dyskinesia in the 6-OHDA model of Parkinson's disease. Involvement of vascular endothelial growth factor and interleukin-1ß. Exp. Neurol. 261, 720–732. https://doi.org/10.1016/j.expneurol.2014.08.019.
Nakaoka, H., Mogi, M., Kan-No, H., Tsukuda, K., Ohshima, K., Wang, X.L., Chisaka, T., Bai, H.Y., Shan, B.S., Kukida, M., Iwanami, J., Horiuchi, M., 2015. Angiotensin II type 2 receptor signaling affects dopamine levels in the brain and prevents binge

eating disorder. J. Renin-Angiotensin-Aldosterone Syst. 16, 749–757. https://doi.org/10.1177/1470320315573680.

Pazos, M.R.R., Mohammed, N., Lafuente, H., Santos, M., Martínez-Pinilla, E., Moreno, E., Valdizan, E., Romero, J., Pazos, A., Franco, R., Hillard, C.J., Alvarez, F.J., Martínez-Orgado, J., 2013. Mechanisms of cannabidiol neuroprotection in hypoxic-ischemic newborn pigs: Role of 5HT1A and CB2 receptors. Neuropharmacology 71, 282–291. https://doi.org/10.1016/j.neuropharm.2013.03.027.

Perez-Lloret, S., Otero-Losada, M., Toblli, J.E., Capani, F., 2017. Renin-angiotensin system as a potential target for new therapeutic approaches in Parkinson's disease. Expert Opin. Investig. Drugs 26, 1163–1173. https://doi.org/10.1080/13543784.2017.1371133.

Pérez-Olives, C., Rivas-Santisteban, R., Lillo, J., Navarro, G., Franco, R., 2021. Recent Advances in the Potential of Cannabinoids for Neuroprotection in Alzheimer's, Parkinson's, and Huntington's Diseases, in: Advances in Experimental Medicine and Biology. Springer, pp. 81–92. https://doi.org/10.1007/978-3-030-57369-0_6.

Pertwee, R.G., Howlett, A.C., Abood, M.E., Alexander, S.P.H., Marzo, V. Di, Elphick, M. R., Greasley, P.J., Hansen, H.S., Kunos, G., 2010. International Union of Basic and Clinical Pharmacology. LXXIX. Cannabinoid Receptors and Their Ligands : Beyond CB 1 and CB 2. Pharmacol. Rev. 62, 588–631. https://doi.org/10.1124/pr.110.003004.588.

Pinna, A., Bonaventura, J., Farré, D., Sánchez, M., Simola, N., Mallol, J., Lluís, C., Costa, G., Baqi, Y., Müller, C.E., Cortés, A., McCormick, P., Canela, E.I., Martínez-Pinilla, E., Lanciego, J.L., Casadó, V., Armentero, M.-T., Franco, R., 2014. L-DOPA disrupts adenosine A(2A)-cannabinoid CB(1)-dopamine D(2) receptor heteromer cross-talk in the striatum of hemiparkinsonian rats: biochemical and behavioral studies. Exp. Neurol. 253, 180–191. https://doi.org/10.1016/j.expneurol.2013.12.021.

Quijano, A., Diaz-Ruiz, C., Lopez-Lopez, A., Villar-Cheda, B., Muñoz, A., Rodriguez-Perez, A.I., Labandeira-Garcia, J.L., 2022. Angiotensin Type-1 Receptor Inhibition Reduces NLRP3 Inflammasome Upregulation Induced by Aging and Neurodegeneration in the Substantia Nigra of Male Rodents and Primary Mesencephalic Cultures. Antioxidants (Basel, Switzerland) 11. https://doi.org/10.3390/ANTIOX11020329.

Reyes-Resina, I., Navarro, G., Aguinaga, D., Canela, E.I., Schoeder, C.T., Załuski, M., Kieć-Kononowicz, K., Saura, C.A., Müller, C.E., Franco, R., 2018. Molecular and functional interaction between GPR18 and cannabinoid CB2 G-protein-coupled receptors. Relevance in neurodegenerative diseases. Biochem. Pharmacol. 157, 169–179. https://doi.org/10.1016/j.bcp.2018.06.001.

Rivas-Santisteban, R., Rodriguez-Perez, A.I., Muñoz, A., Reyes-Resina, I., Labandeira-García, J.L., Navarro, G., Franco, R., 2020. Angiotensin AT1 and AT2 receptor heteromer expression in the hemilesioned rat model of Parkinson's disease that increases with levodopa-induced dyskinesia. J. Neuroinflammation 17. https://doi.org/10.1186/s12974-020-01908-z.

Rivas-Santisteban, R., Lillo, J., Muñoz, A., Rodríguez-Pérez, A.I., Labandeira-García, J.L., Navarro, G., Franco, R., 2021. Novel Interactions Involving the Mas Receptor Show Potential of the Renin-Angiotensin system in the Regulation of Microglia Activation: Altered Expression in Parkinsonism and Dyskinesia. Neurotherapeutics 18, 998–1016. https://doi.org/10.1007/S13311-020-00986-4.

Rodriguez-Perez, A.I., Sucunza, D., Pedrosa, M.A., Garrido-Gil, P., Kulisevsky, J., Lanciego, J.L., Labandeira-Garcia, J.L., 2018. Angiotensin Type 1 Receptor Antagonists Protect Against Alpha-Synuclein-Induced Neuroinflammation and Dopaminergic Neuron Death. Neurotherapeutics 15, 1063–1081. https://doi.org/10.1007/S13311-018-0646-Z.

Rodriguez-Perez, A.I., Garrido-Gil, P., Pedrosa, M.A., Garcia-Garrote, M., Valenzuela, R., Navarro, G., Franco, R., Labandeira-Garcia, J.L., 2020. Angiotensin type 2 receptors: Role in aging and neuroinflammation in the substantia nigra. Brain Behav. Immun. 87, 256–271. https://doi.org/10.1016/j.bbi.2019.12.011.

Royea, J., Lacalle-Aurioles, M., Trigiani, L.J., Fermigier, A., Hamel, E., 2020. AT2R's (Angiotensin II Type 2 Receptor's) Role in Cognitive and Cerebrovascular Deficits in a Mouse Model of Alzheimer Disease. Hypertens. (Dallas, Tex. 1979) 75, 1464–1474. https://doi.org/10.1161/HYPERTENSIONAHA.119.14431.

Rozenfeld, R., Gupta, A., Gagnidze, K., Lim, M.P., Gomes, I., Lee-Ramos, D., Nieto, N., Devi, L.A., 2011. AT_1R-CB_1R heteromerization reveals a new mechanism for the pathogenic properties of angiotensin II. EMBO J. 30, 2350–2363. https://doi.org/10.1038/emboj.2011.139.

Ruiz-Calvo, A., Bajo-Grañeras, R., Maroto, I.B., Zian, D., Grabner, G.F., García-Taboada, E., Resel, E., Zechner, R., Zimmermann, R., Ortega-Gutiérrez, S., Galve-Roperh, I., Bellocchio, L., Guzmán, M., 2019. Astroglial monoacylglycerol lipase controls mutant huntingtin-induced damage of striatal neurons. Neuropharmacology 150, 134–144. https://doi.org/10.1016/j.neuropharm.2019.03.027.

Sam, A.H., Salem, V., Ghatei, M.A., 2011. Rimonabant: From RIO to Ban. J. Obes. 2011, 432607 https://doi.org/10.1155/2011/432607.

Sierra, S., Luquin, N., Rico, A.J., Gómez-Bautista, V., Roda, E., Dopeso-Reyes, I.G., Vázquez, A., Martínez-Pinilla, E., Labandeira-García, J.L., Franco, R., Lanciego, J.L., 2015. Detection of cannabinoid receptors CB1 and CB2 within basal ganglia output neurons in macaques: changes following experimental parkinsonism. Brain Struct. Funct. 220, 2721–2738. https://doi.org/10.1007/s00429-014-0823-8.

Simon, V., Cota, D., 2017. Mechanisms in endocrinology: Endocannabinoids and metabolism: Past, present and future. Eur. J. Endocrinol. https://doi.org/10.1530/EJE-16-1044.

Singh, M.R., Vigh, J., Amberg, G.C., 2021. Angiotensin-II Modulates GABAergic Neurotransmission in the Mouse Substantia Nigra. eNeuro 8. https://doi.org/10.1523/ENEURO.0090-21.2021.

Uberti, M.A., Hall, R.A., Minneman, K.P., 2003. Subtype-specific dimerization of alpha 1-adrenoceptors: effects on receptor expression and pharmacological properties. Mol. Pharmacol. 64, 1379–1390. https://doi.org/10.1124/MOL.64.6.1379.

Urmila, A., Rashmi, P., Nilam, G., Subhash, B., 2021. Recent Advances in the Endogenous Brain Renin-Angiotensin System and Drugs Acting on It. J. Renin-Angiotensin-Aldosterone Syst. 2021, 9293553. https://doi.org/10.1155/2021/9293553.

Velayudhan, L., Van Diepen, E., Marudkar, M., Hands, O., Suribhatla, S., Prettyman, R., Murray, J., Baillon, S., Bhattacharyya, S., 2014. Therapeutic potential of cannabinoids in neurodegenerative disorders: a selective review. Curr. Pharm. Des. 20, 2218–2230.

Villar-Cheda, B., Dominguez-Meijide, A., Valenzuela, R., Granado, N., Moratalla, R., Labandeira-Garcia, J.L., 2014. Aging-related dysregulation of dopamine and angiotensin receptor interaction. Neurobiol. Aging 35, 1726–1738. https://doi.org/10.1016/j.neurobiolaging.2014.01.017.

Winkler, C., Kirik, D., Björklund, A., Cenci, M.A., 2002. L-DOPA-induced dyskinesia in the intrastriatal 6-hydroxydopamine model of parkinson's disease: relation to motor and cellular parameters of nigrostriatal function. Neurobiol. Dis. 10, 165–186. https://doi.org/10.1006/nbdi.2002.0499.

Wright, J.W., Harding, J.W., 2013. The brain renin-angiotensin system: a diversity of functions and implications for CNS diseases. Pflugers Arch. 465, 133–151. https://doi.org/10.1007/S00424-012-1102-2.

Yang, J., Gao, Y., Duan, Q., Qiu, Y., Feng, S., Zhan, C., Huang, Y., Zhang, Y., Ma, G., Nie, K., Wang, L., 2022. Renin-angiotensin system blockers affect cognitive decline in Parkinson's disease: The PPMI dataset. Parkinsonism Relat. Disord. 105, 90–95. https://doi.org/10.1016/J.PARKRELDIS.2022.10.019.

Zeissler, M.-L., Eastwood, J., McCorry, K., Hanemann, O.C., Zajicek, J.P., Carroll, C.B., 2016. Δ-9-tetrahydrocannabinol protects against MPP+ toxicity in SH-SY5Y cells by restoring proteins involved in mitochondrial biogenesis. Oncotarget 7, 46603–46614. https://doi.org/10.18632/oncotarget.10314.

Zhou, Z., Zhou, X., Xiang, Y., Zhao, Y., Pan, H., Wu, J., Xu, Q., Chen, Y., Sun, Q., Wu, Xinyin, Zhu, J., Wu, Xuehong, Li, J., Yan, X., Guo, J., Tang, B., Lei, L., Liu, Z., 2022. Subtyping of early-onset Parkinson's disease using cluster analysis: A large cohort study. Front. Aging Neurosci. 14 https://doi.org/10.3389/FNAGI.2022.1040293.